PNAS RESEARCH ARTICLE | BIOCHEMISTRY OPEN ACCESS

The role of GTP hydrolysis by EF-G in ribosomal translocation

Gillian Rexroad[a,b], John Paul Donohue[a,b], Laura Lancaster[a,b], and Harry F. Noller[a,b,1]

Contributed by Harry Noller; received July 20, 2022; accepted September 27, 2022; reviewed by Dmitri Ermolenko, Rachel Green, and Peter Cornish

Translocation of transfer RNA (tRNA) and messenger RNA (mRNA) through the ribosome is catalyzed by the GTPase elongation factor G (EF-G) in bacteria. Although guanosine-5'-triphosphate (GTP) hydrolysis accelerates translocation and is required for dissociation of EF-G, its fundamental role remains unclear. Here, we used ensemble Förster resonance energy transfer (FRET) to monitor how inhibition of GTP hydrolysis impacts the structural dynamics of the ribosome. We used FRET pairs S12-S19 and S11-S13, which unambiguously report on rotation of the 30S head domain, and the S6-L9 pair, which measures intersubunit rotation. Our results show that, in addition to slowing reverse intersubunit rotation, as shown previously, blocking GTP hydrolysis slows forward head rotation. Surprisingly, blocking GTP hydrolysis completely abolishes reverse head rotation. We find that the S13-L33 FRET pair, which has been used in previous studies to monitor head rotation, appears to report almost exclusively on intersubunit rotation. Furthermore, we find that the signal from quenching of 3′-terminal pyrene–labeled mRNA, which is used extensively to follow mRNA translocation, correlates most closely with reverse intersubunit rotation. To account for our finding that blocking GTP hydrolysis abolishes a rotational event that occurs after the movements of mRNA and tRNAs are essentially complete, we propose that the primary role of GTP hydrolysis is to create an irreversible step in a mechanism that prevents release of EF-G until both the tRNAs and mRNA have moved by one full codon, ensuring productive translocation and maintenance of the translational reading frame.

ribosome | FRET | translation | frameshifting

Significance

Using ensemble FRET, we measured the effects of inhibition of GTP hydrolysis on rotational movements of the 30S ribosomal subunit and of the head domain of the 30S subunit during ribosomal translocation. Surprisingly, we find that blockage of GTP hydrolysis by the elongation factor G (EF-G) specifically abolishes reverse rotation of the head domain of the small ribosomal subunit, an event that occurs after translocation of the transfer RNA and messenger RNA is essentially complete. We propose that the principal role of GTP hydrolysis is to ensure that EF-G is not released from the ribosome until completion of each round of translocation, which guards against slippage of the translational reading frame.

Following formation of each peptide bond, the messenger RNA (mRNA) and transfer RNA (tRNA) are translocated through the ribosome to advance the message by one codon. This process is catalyzed by a GTPase, the elongation factor G (EF-G) (1). Translocation is coupled to several large-scale conformational changes in the ribosome, including overall rotation of the 30S subunit relative to the 50S subunit (2, 3) and rotation of the head domain of the 30S subunit (4, 5). Intersubunit rotation, which can occur spontaneously (6), is coupled to translocation of the acceptor ends of the tRNAs on the 50S subunit (7). Rotation of the 30S head domain, which requires participation of EF-G (8), is coupled to translocation of the anticodon ends of the tRNAs and their associated mRNA codons on the 30S subunit (5, 9–11).

While guanosine-5'-triphosphate (GTP) hydrolysis by EF-G is not required for a single round of translocation, as shown originally by Kaziro and co-workers (12) using the nonhydrolyzable GTP analog GDPNP, it is required for the multiple turnover reaction as it is essential for dissociation of EF-G (12–15). Additionally, kinetic experiments show that GTP hydrolysis both precedes and accelerates translocation, suggesting that it plays a role in driving tRNA movement (16). The physical basis of this acceleration, however, has been debated. It has been proposed that GTP hydrolysis induces a conformational change in EF-G that either actively moves the tRNAs through a "power stroke" (16–21) or induces a structural rearrangement in the ribosome that facilitates tRNA movement (2, 13, 17, 22–26). Others have proposed that GTP hydrolysis is coupled to tRNA-mRNA movement in a Brownian ratchet mechanism of translocation, in which movement is driven by thermal energy and EF-G acts as a pawl to prevent backward movement (5, 6, 27–33). Although EF-G accelerates translocation by at least 10,000-fold (16, 34), GTP hydrolysis contributes only about a 50-fold rate enhancement (13, 14, 16, 35). Thus, it is evident that driving tRNA movement is not the primary role of GTP hydrolysis.

Efforts to dissect the impact of GTP hydrolysis on the kinetics of the large-scale structural dynamics of the ribosome have used FRET-based approaches to follow intersubunit rotation and rotation of the head domain of the 30S subunit (31, 36–38). While the effects of GTP hydrolysis on intersubunit rotation have been measured directly using the S6-L9 FRET pair (7, 36–39), 30S head rotation has been inferred indirectly from changes in FRET efficiencies from fluorescent labels attached to sites that undergo more than one mode of movement (31, 37, 38). Here, we clarify how inhibition of GTP hydrolysis affects the kinetics of head rotation using the previously described FRET pairs

Author affiliations: [a]Center for Molecular Biology of RNA, University of California, Santa Cruz, CA 95064; and [b]Department of Molecular, Cell and Developmental Biology, University of California, Santa Cruz, CA 95064

Author contributions: G.R. and H.F.N. designed research; G.R. and L.L. performed research; G.R., J.P.D., L.L., and H.F.N. analyzed data; and G.R., L.L., and H.F.N. wrote the paper.

Reviewers: D.E., University of Rochester School of Medicine and Dentistry; R.G., Johns Hopkins University School of Medicine; and P.C., University of Missouri.

The authors declare no competing interest.

[1]To whom correspondence may be addressed. Email: nollerharry@gmail.com.

This article contains supporting information online at http://www.pnas.org/lookup/suppl/doi:10.1073/pnas.2212502119/-/DCSupplemental.

Published October 25, 2022.

S12(Alx488)-S19(Alx568) and S11(Alx488)-S13(Alx568) (8). These constructs each report directly and unambiguously on rotation of the 30S head domain, measuring energy transfer between one fluor in the head domain and another in the body domain. In parallel, we monitor intersubunit rotation using the previously reported S6-L9 FRET pair (7).

We observe that blocking GTP hydrolysis modestly inhibits forward head rotation and slows reverse intersubunit rotation, as shown previously (36). Surprisingly, we find that blocking GTP hydrolysis completely abolishes reverse rotation of the 30S head domain. We also show that the S13-L33 Förster resonance energy transfer (FRET) pair previously used for monitoring 30S head rotation (37) appears to report mainly on intersubunit rotation and has thus masked the effects of GTP hydrolysis on reverse head rotation. We additionally find that the signal in a widely used mRNA quenching assay (40), in which a 3′-terminal pyrene is quenched upon translocation by one codon, appears to be connected to reverse intersubunit rotation. Based on our finding that blockage of GTP hydrolysis abolishes a rotational event that occurs after the movements of mRNA and tRNAs are essentially complete, we propose that the primary role of GTP hydrolysis is to enforce the accuracy and completion of each round of translocation.

Results

Monitoring Conformational Dynamics in the Ribosome with FRET. To monitor how GTP hydrolysis by EF-G affects the structural dynamics of the ribosome during translocation, we used ensemble FRET stopped-flow kinetics. Forward and reverse 30S head rotation were followed using the S12-S19 and S11-S13 FRET pairs (8) (Fig. 1 *A* and *B*). The S6(Cy5)-L9(Cy3) FRET pair (7) was used to follow intersubunit rotation (Fig. 1*C*). We also constructed the S13(Atto540Q)-L33(Alx488) FRET pair (*SI Appendix*, Fig. S1) to directly compare our results to previous reports that used this pair to monitor 30S head rotation (37).

A pretranslocation hybrid-state complex was formed with labeled ribosomes, a 39-nucleotide mRNA, deacylated elongator $tRNA^{Met}$ bound in the P/E state and NAc-Met-Val-$tRNA^{Val}$ in the A/P state (*Materials and Methods*). EF-G in the presence of GTP or various GTP analogs was rapidly delivered to the pretranslocation complex, and the fluorescence signal was recorded over a single round of translocation.

Intersubunit Rotation Proceeds in the Absence of GTP Hydrolysis. We first investigate the effects of inhibition of GTP hydrolysis on intersubunit rotation using the S6-L9 FRET pair (7) (Fig. 1*C*) in order to directly compare these rates with those from our head rotation reporters, described below. Since our pretranslocation complex has already undergone forward intersubunit rotation, we measure the rate constant of reverse intersubunit rotation by following the increase in acceptor fluorescence (Fig. 2*A*). With wild-type EF-G and GTP, the apparent rate constant for reverse intersubunit rotation is ~4.3 s^{-1} at 22° (Table 1), in close agreement with that reported previously (36). Although this rate is slower than that reported by Belardinelli et al. (42) for the same pair (~47 s^{-1}), this difference can be explained by the lower temperature and concentration of EF-G (10-fold molar excess over ribosomes) used in our study compared to the conditions used by Belardinelli et al. (37° and 80-fold excess).

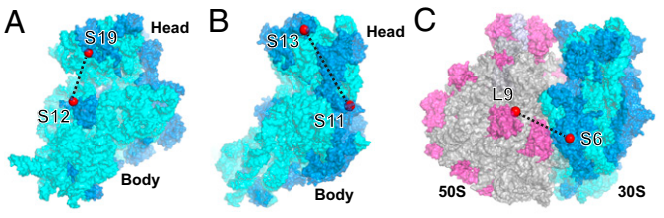

Fig. 1. Positions of FRET pairs used to monitor ribosome dynamics. (*A*) S12-S19 and (*B*) S11-S13 FRET pairs report on rotation of the 30S head domain (8). (*C*) S6-L9 FRET pair reports on intersubunit rotation (7). Ribosomal components are 16S ribosomal RNA (rRNA) (cyan), 30S proteins (blue), 23S rRNA (gray), 5S rRNA (light blue), and 50S proteins (magenta). Positions of fluorophores are indicated by red spheres (PDB 4V9D) (41).

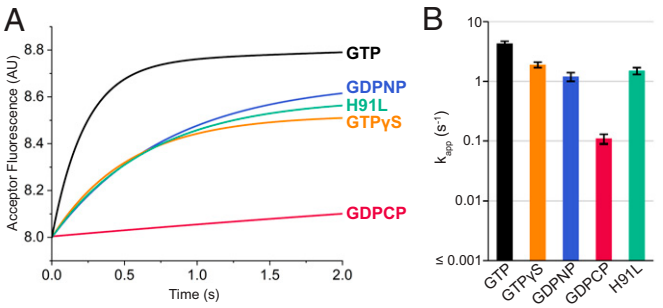

Fig. 2. Effects of inhibition of GTP hydrolysis on reverse intersubunit rotation. (*A*) Reverse intersubunit rotation was monitored using the S6-L9 FRET pair (7). At $t = 0$, a pretranslocation complex was rapidly mixed with either EF-G·GTP (GTP), EF-G·GDPNP (GDPNP), EF-G·GDPCP (GDPCP), EF-G·GTPγS (GTPγS), or EF-G(H91L)·GTP (H91L), and changes in ensemble FRET efficiency were measured using a stopped-flow fluorometer (*Materials and Methods*). Curves are single-exponential functions fitted to the experimental traces (*SI Appendix*, Fig. S3). With the exception of GDPCP, inhibiting GTP hydrolysis had only modest effects on the rate of reverse intersubunit rotation. (*B*) Pseudo-first order rate constants for the traces from panel *A* (*SI Appendix*, Fig. S3 and Table 1). Error bars represent SD about the mean. AU, arbitrary unit.

To inhibit hydrolysis, we began by substituting GTP with the nonhydrolyzable analogs GDPNP and GDPCP and the slowly hydrolyzed GTP analog GTPγS. We also blocked GTP hydrolysis using EF-G carrying the GTPase-defective mutation H91L, identified previously in a screen for dominant-lethal mutations in EF-G (43). We tested the ribosome-dependent GTP hydrolysis activity of EF-G (H91L) and found that it was undetectable over background, even after several minutes at 37° (*SI Appendix*, Fig. S2). In parallel, we tested the EF-G mutant H91A and also found it to be completely defective in GTP hydrolysis, in agreement with previous findings (13, 44).

Inhibition of GTP hydrolysis using the analogs GDPNP, GDPCP, and GTPγS or mutant EF-G(H91L) generally caused only modest (approximately two- to fourfold) decreases in the rate of reverse intersubunit rotation, except for the case of GDPCP, which reduced the rate by 39-fold (Fig. 2 and Table 1), in general agreement with previous reports (36, 37). These results show that although GTP hydrolysis modestly accelerates reverse intersubunit rotation, it is not required.

Forward Rotation of the 30S Head Domain Proceeds in the Absence of GTP Hydrolysis. We next ask how inhibition of GTP hydrolysis affects the rates of rotation of the 30S subunit head domain. Upon delivery of EF-G·GTP to a pretranslocation complex containing the S12-S19 FRET pair, the FRET efficiency decreased with an apparent rate constant of 23 s^{-1}, indicating rapid forward rotation of the 30S subunit head domain (Fig. 3*A* and Table 1). This was followed by a slower (4.9 s^{-1}) increase in FRET efficiency, corresponding to reverse head rotation (8). Using ribosomes reconstituted with the S11-S13 FRET pair, similar forward and reverse rotational rate constants were observed (Fig. 3*B* and Table 1), but changes in FRET were anticorrelated with the S12-S19 pair, as expected (8).

Table 1. Effects of inhibition of GTP hydrolysis on the rates of intersubunit and 30S head rotation*

	Reverse intersubunit rotation	Forward 30S head rotation		Reverse 30S head rotation	
	S6·L9	S11·S13	S12·S19	S11·S13	S12·S19
GTP	4.3 ± 0.4	25 ± 10	23 ± 4	4.3 ± 0.6	4.9 ± 0.5
GTPγS	1.9 ± 0.2	2.3 ± 0.2	2.07 ± 0.07	0.24 ± 0.01	0.16 ± 0.03
GDPNP	1.2 ± 0.2	0.05 ± 0.01	0.059 ± 0.004	$<10^{-3}$	$<10^{-3}$
GDPCP	0.11 ± 0.02	0.25 ± 0.03	0.30 ± 0.08	$<10^{-3}$	$<10^{-3}$
H91L	1.5 ± 0.2	2.5 ± 0.4	2.2 ± 0.3	$<10^{-3}$	$<10^{-3}$

*Rotational rates represent apparent rate constants, given in s^{-1}, derived from single- or double-exponential functions fitted to the experimental traces (*SI Appendix*, Figs. S3–S5 and Figs. 2 and 3). Errors represent SD about the mean.

Substituting GTP with the slowly hydrolyzed GTP analog GTPγS slowed the rate of forward head rotation by 11-fold, and the nonhydrolyzable GTP analogs GDPNP and GDPCP more strongly reduced the rate, by 450-fold and 90-fold, respectively (Figs. 3 and 4*A* and Table 1). Surprisingly, the GTPase-deficient EF-G mutant H91L slowed forward head rotation substantially less (10-fold) than did the nonhydrolyzable analogs (Figs. 3 and 4*A*). Our findings are consistent with previous biochemical evidence showing slow single-round translocation in the absence of GTP hydrolysis (12, 13, 16) and structural studies showing 30S head rotation in the presence of GDPNP or GDPCP (10, 45).

Blocking GTP Hydrolysis Abolishes Reverse Rotation of the 30S Head Domain. Rates of reverse head rotation were obtained from the second phase of the traces in Fig. 3, where changes in FRET efficiency reversed direction upon reversal of 30S head rotation (Fig. 3). When GTP was replaced with the slowly hydrolyzed GTPγS, the rate of reverse head rotation was slowed by 23-fold, in general agreement with a previous report (37). This demonstrates that slowing the rate of GTP hydrolysis impacts reverse head rotation to a greater degree than it affects forward head rotation (11-fold), as suggested previously (37). But when GTP hydrolysis was blocked using the nonhydrolyzable GTP analogs GDPNP and GDPCP or the H91L mutant form of EF-G, reverse head rotation was undetectable (Figs. 3 and 4). These results show that, in contrast to forward head rotation or intersubunit rotation, blockage of GTP hydrolysis abolishes reverse head rotation.

The S13-L33 FRET Pair Primarily Reports on Intersubunit Rotation. Several of our observations involving 30S head rotation differ from those reported previously. For example, it was previously reported that forward head rotation was not observable in the presence of the nonhydrolyzable analogs GDPNP and GDPCP and that reverse head rotation was slowed but not abolished (37). This contrasts with our findings of slowed forward head rotation but complete blockage of reverse head rotation with these analogs. In the study by Belardinelli et al. (37), 30S head rotation was inferred indirectly using a FRET pair with labels on proteins S13 in the 30S head domain and L33 on the 50S subunit. Since this pair contains labels on both subunits, changes in FRET efficiency could be the result of distance changes due to intersubunit rotation, head rotation, or some combination of both. To test this possibility, we directly compared the results from our S12-S19 and S11-S13 pairs with those from the S13-L33 pair.

Upon delivery of EF-G·GTP to a labeled pretranslocation complex containing the S13-L33 FRET pair, we observed a biphasic increase in the fluorescence of Alexa488 (Fig. 5*A*), similar to the observations of Belardinelli et al. (37). When GTP was replaced with GDPNP or the mutant EF-G(H91L) was used, we continued to observe fluorescence changes, although with decreased amplitudes and modestly (approximately two- to threefold) decreased rates (Fig. 5*A* and *SI Appendix*, Table S1). These results contrast with those obtained with the S11-S13 and S12-S19 pairs, which show complete blockage of reverse head rotation (Figs. 3 and 4). The persistence of large changes in FRET

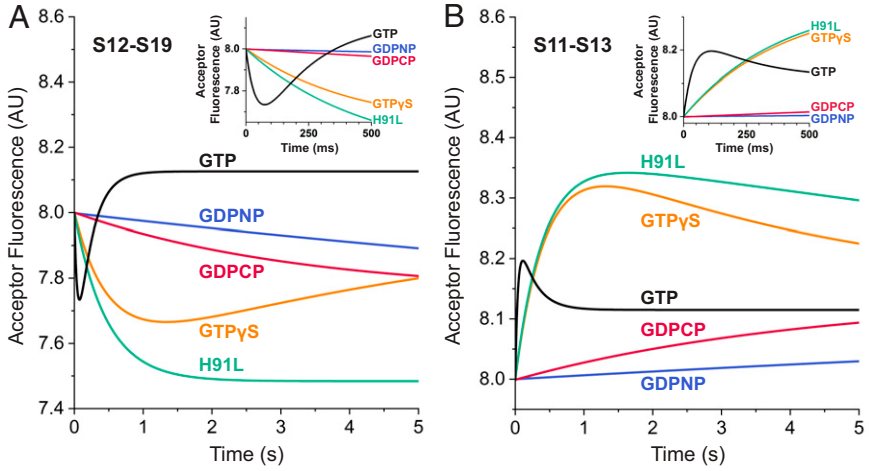

Fig. 3. Effects of inhibition of GTP hydrolysis on 30S head rotation. Forward and reverse 30S head rotation were monitored with two anticorrelated FRET pairs (8). (*A*) For the S12-S19 FRET pair, decreasing and increasing acceptor fluorescence indicate forward and reverse rotation, respectively. (*B*) For the S11-S13 FRET pair, increasing and decreasing acceptor fluorescence indicate forward and reverse rotation, respectively. Experimental traces were fitted to double-exponential functions (*SI Appendix*, Figs. S4 and S5 and Table 1). Insets show expanded views of the first 500 ms. AU, arbitrary unit.

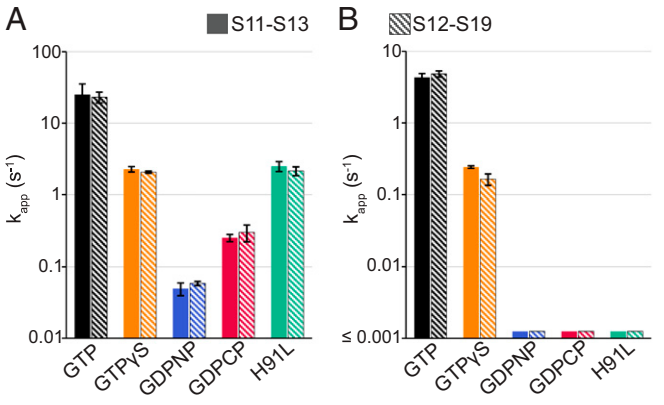

Fig. 4. Reverse head rotation is abolished in the absence of GTP hydrolysis. Apparent rate constants for (*A*) forward and (*B*) reverse head rotation were obtained from fitting the traces from Fig. 3 to double-exponential functions (*SI Appendix*, Figs. S4 and S5 and Table 1). Error bars represent SD about the mean.

efficiency from the S13-L33 pair under two different conditions, which in our hands abolish reverse head rotation, appears to indicate that the S13-L33 pair is an unreliable reporter for 30S head rotation.

As can be seen in Fig. 5*B*, the apparent rate constants for the S13-L33 FRET pair for the GTP, GDPNP, and H91L conditions correlate most closely with those for reverse intersubunit rotation monitored using the S6-L9 FRET pair and differ from those measured directly for either forward or reverse head rotation. We conclude that the signal from the S13-L33 pair observed with GDPNP and H91L is mainly attributable to reverse intersubunit rotation, which could account for the apparent discrepancies between the observations made using the different FRET reporters.

mRNA Quenching Correlates Most Closely with Reverse Intersubunit Rotation. Finally, we asked which of the different ribosomal rotational events correlates most closely with quenching of the signal from a pyrene-labeled mRNA (40), one of the most widely used kinetic measures of mRNA translocation. In this assay, the signal from a pyrene at position +9 (relative to the first nucleotide of the P-site codon at position +1) at the 3′ end of a 24-nucleotide mRNA is quenched, following a bimodal decay, upon translocation by one codon to the +6 position (Fig. 6*A*). We observe that quenching rates are decreased by only about two- to threefold upon inhibition of GTP hydrolysis, except in the case of GDPCP, which reduced the rate more substantially (11-fold) (Fig. 6*A*), in general agreement with the findings of Salsi et al. (31).

Most importantly, mRNA quenching proceeds under conditions in which reverse head rotation is abolished (H91L, GDPNP, GDPCP) (Fig. 6). Previously, the quenching signal has been attributed to reverse head rotation due to the similarity between the apparent rate constants of reverse head rotation and the fast phase of mRNA quenching (8). However, the persistence of mRNA quenching under conditions where reverse head rotation is abolished shows that mRNA quenching cannot be caused by reverse head rotation. Finally, the rates of mRNA quenching and reverse body rotation are impacted to similar extents under each condition (Fig. 6*B*), suggesting that these events are connected.

Discussion

GTP hydrolysis by EF-G has previously been proposed to drive tRNA movement (16, 46). Some investigators have proposed that hydrolysis is coupled to a conformational change in EF-G that either actively moves the tRNAs and mRNA in a "power stroke" (17, 19, 20) or induces a conformational change in the ribosome that provides the energy for tRNA and/or mRNA movement (13, 17, 22–26). Others have suggested a Brownian ratchet mechanism driven by thermal energy in which EF-G acts as a pawl to prevent backward movement of the tRNAs (5, 6, 27–33). Still others have suggested mechanisms that combine elements of both (18, 21, 25, 26, 47). However, EF-G accelerates translocation by over ∼10,000-fold (16, 35), while GTP hydrolysis contributes only about a 30- to 50-fold increase in rate (13, 14, 16, 35). Although the latter rate increase may well be explained by such models, we conclude that the principal role of GTP hydrolysis is not to drive tRNA or mRNA movement. Indeed, it has been argued that EF-G not only does not *push* the tRNAs through the ribosome, but actually *restrains* their movement (48).

In their pioneering studies showing a complete round of translocation in the presence of GDPNP, Kaziro and coworkers (12, 49) suggested that the primary role of GTP hydrolysis is to enable cycling of EF-G on and off the ribosome. The strict requirement of GTP hydrolysis for dissociation of EF-G (12–15) strongly suggests that the role of GTP hydrolysis must indeed be linked to EF-G occupancy; yet, merely facilitating release of EF-G would not seem to justify such a costly expenditure of energy. Finally, EF-G remains bound to the ribosome long after GTP hydrolysis, which

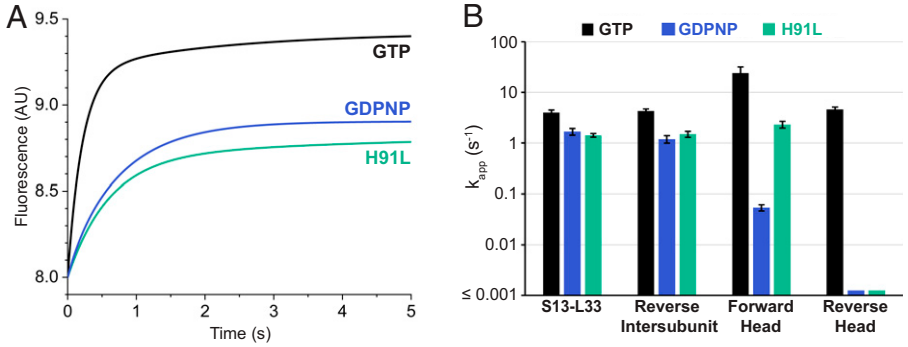

Fig. 5. The S13·L33 FRET pair likely reports primarily on reverse intersubunit rotation. (*A*) A pretranslocation complex containing ribosomes with the S13(Atto540Q)-L33(Alexa488) FRET pair was combined with either EF-G·GTP, EF-G·GDPNP, or EF-G(H91L)·GTP in a stopped-flow fluorometer. The fluorescence signal from Alexa488 was monitored over a single round of translocation. (*B*) The weighted average apparent rate constants (k_{app}) for the biphasic FRET changes from the S13-L33 FRET pair for GTP, GDPNP, and H91L conditions (*SI Appendix*, Table S1 and *SI Methods*) correlate most closely with the respective rates of reverse intersubunit rotation monitored using the S6-L9 FRET pair and differ from those measured directly for either forward or reverse head rotation (Table 1). AU, arbitrary unit.

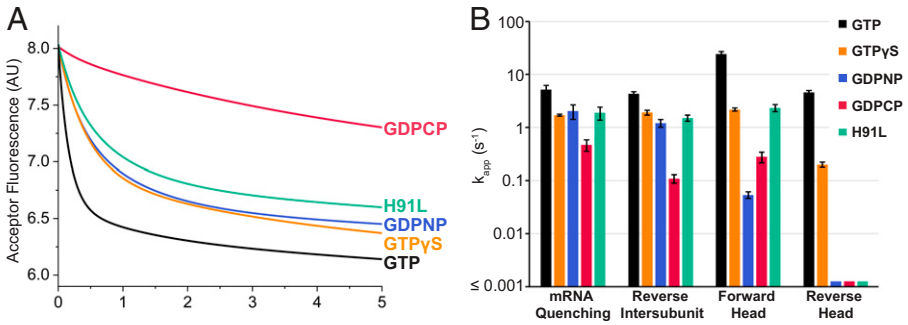

Fig. 6. mRNA quenching correlates most closely with reverse intersubunit rotation. (*A*) Translocation was monitored by quenching of a fluorophore attached to the 3′ end (position +9) of a 24-nt mRNA (40). The biphasic experimental traces (*SI Appendix*, Fig. S7) were fit to double-exponential curves. (*B*) Weighted average apparent rate constants (k_{ave}) for mRNA quenching (*SI Appendix, SI Methods*) correspond most closely to those for reverse intersubunit rotation (Table 1 and *SI Appendix*, Table S2). AU, arbitrary unit.

occurs rapidly upon EF-G binding (23), pointing to the importance of the persistence of EF-G on the ribosome. GTP hydrolysis must, therefore, serve some other crucial function.

Here, we sought to clarify how blocking GTP hydrolysis affects structural rearrangements that occur in the ribosome during translocation using FRET pairs that directly report on 30S head rotation. Surprisingly, we find that the single step that requires GTP hydrolysis is reverse rotation of the 30S subunit head domain. That both dissociation of EF-G and reverse head rotation require GTP hydrolysis implies that they are linked. Thus, EF-G remains on the ribosome throughout forward head rotation and completion of movement of tRNA and mRNA (Fig. 7), consistent with recent time-resolved cryo-EM structures of translocation intermediates (21, 32).

But why must EF-G remain on the ribosome during this time? The most serious error that can occur during protein synthesis is shifting of the translational reading frame, which causes incorrect reading of all subsequent codons, including out-of-frame stop codons, thus creating potentially toxic truncated polypeptide products. The reading frame is most vulnerable to frameshifting during movement, when neither of the two codon-anticodon duplexes is stabilized by their ribosomal binding sites. During movement of the duplexes, EF-G acts to maintain the reading frame by contacting the minor groove of the A-site codon-anticodon duplex and stabilizing it until movement is complete (9, 11, 43, 48, 50–52). The vulnerability of the reading frame during movement has been captured in

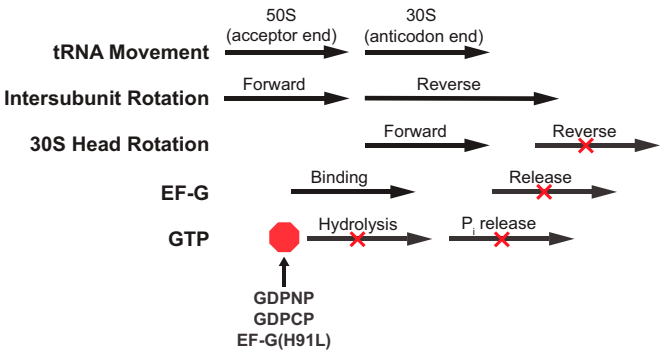

Fig. 7. Effects of blocking GTP hydrolysis on events during translocation. Blocking GTP hydrolysis specifically abolishes reverse rotation of the 30S subunit head domain (Figs. 3 and 4), likely due to inhibition of release of EF-G, which requires release of P_i (12–15). Arrows indicate proposed order of events during a single round of translocation. Red octagon symbol indicates blockage of GTP hydrolysis by GDPNP, GDPCP, or EF-G(H91L). Red X marks indicate steps abolished by blockage of GTP hydrolysis.

the structures of two translocation intermediates undergoing −1 and +1 frameshifting events, respectively (45, 48).

We propose that the principal role of GTP hydrolysis is to create a checkpoint to ensure that the mRNA and tRNAs have translocated by one full codon before EF-G is released. Since GTP hydrolysis occurs much earlier in the sequence of events, the actual signal for release of EF-G is likely release of inorganic phosphate (P_i). Consistent with this is the finding that inhibiting Pi release blocks multipleturnover translocation (15). If dissociation of EF-G is required for reverse rotation of the 30S head domain, it would explain why GTP hydrolysis is required for reverse head rotation. By preventing release of EF-G until the duplex has moved by precisely one codon, GTP hydrolysis enforces maintenance of the reading frame and a round of productive translocation, justifying the expenditure of this chemical energy.

Our model is consistent with a recent time-resolved cryo-EM structural study of translocation dynamics by Korostelev and coworkers (33). The authors infer that GTP hydrolysis is used as a switch controlling the ability of EF-G to bind and leave the ribosome rather than for driving tRNA movement. They similarly conclude that EF-G remains bound to the ribosome until reaching a final stage of 30S head rotation to support the tRNA-mRNA duplex and prevent frameshifting. Our results now provide direct kinetic evidence that reveals a fundamental connection between GTP hydrolysis and reverse head rotation. Our results are also in agreement with the finding that late steps in translocation on mammalian ribosomes are stalled in the absence of GTP hydrolysis (53). However, that same study concluded that late steps of translocation on bacterial ribosomes are merely slowed when GTP hydrolysis is abolished, in contrast to our findings. We suspect that use of a FRET pair containing labels on A-site tRNA and protein uS13, which would be sensitive to both tRNA movement and 30S head rotation, may have obscured the effect of blocking GTP hydrolysis on reverse head rotation. Our results demonstrate that GTP hydrolysis is required for resolving late steps in bacterial translocation, just as in the mammalian mechanism.

Given the seriousness of losing the translational reading frame, it should not be surprising to learn that other and perhaps even all translational GTPases are in some way involved in guarding against frameshifting. Initiation factor IF2 helps to ensure selection of the initiator tRNA at the start codon, establishing the reading frame at the outset of translation (54). Elongation factor EF-Tu helps to maintain the reading frame (55, 56) by preventing binding of noncognate tRNAtRNAs to the A site (57, 58), which can result in frameshifting (59). And release factor RF3 has been shown to elicit termination following miscoding and frameshifting events (60, 61), protecting the

cell against miscoded proteins. It thus seems possible that the seemingly costly expenditure of GTP throughout all steps of protein synthesis may have a common basis in avoiding the dangers of translational frameshifting.

Materials and Methods

Materials. Doubly labeled S12-S19 and S11-S13 70S ribosomes were constructed by *in vitro* reconstitution of 30S subunits from 16S rRNA, and 20 purified ribosomal proteins, including fluorescently labeled S12(Alx488) and S19(Alx568) or S11(Alx488) and S13(Alx568), followed by association with natural 50S subunits. Doubly labeled S6-L9 ribosomes were purified by reconstituting 30S (ΔS6) and 50S (ΔL9) subunits isolated from S6 and L9 deletion strains, respectively, with fluorescently labeled S6(Cy5) and L9(Cy3). Doubly labeled 70S-S13-L33 ribosomes were purified by reconstituting 30S (ΔS13) and 50S (ΔL33) isolated from S13 and L33 deletion strains, respectively, with fluorescently labeled S13(Atto540Q) and L33(Alx488).

Methods. Pretranslocation complexes were formed from fluorescently labeled ribosomes, a 39-nt transcribed mRNA, $tRNA^{Met}$ in the P/E state, and N-Ac-Met-Val-$tRNA^{Val}$ in the A/P state. S6-L9 ribosomes were used to measure intersubunit rotation, and S12-S19 and S11-S13 ribosomes were used to measure 30S head rotation. Overall translocation rates were measured using a 24-nt mRNA containing a 3′-terminal pyrene. Fluorescence changes over a single round of translocation following rapid mixing of the pretranslocation complex with EF-G and GTP (or nonhydrolyzable analog) were monitored using an Applied Photophysics SX20 stopped-flow fluorometer at 22 °C. GTP hydrolysis was blocked using the nonhydrolyzable analogs GDPNP and GDPCP or the H91L mutant of EF-G or slowed using the GTP analog GTPγS. Fusidic acid was introduced together with EF-G and GTP when used. Fluorescence traces were fit to single- or double-exponential functions to obtain apparent rate constants. Inhibition of hydrolysis of α-[^{32}P]-GTP was measured by thin-layer chromatography. Full details of materials and methods are presented in the *SI Appendix*.

Data, Materials, and Software Availability. All study data are included in the article and/or supporting information.

ACKNOWLEDGMENTS. We thank Clive Bagshaw for helpful discussions and Rachel Green for providing the S13 deletion strain. This work was funded by National Institutes of Health grant R35-GM118156 to H.F.N.

1. S. L. Gupta, J. Waterson, M. L. Sopori, S. M. Weissman, P. Lengyel, Movement of the ribosome along the messenger ribonucleic acid during protein synthesis. *Biochemistry* **10**, 4410–4421 (1971).
2. J. Frank, R. K. Agrawal, A ratchet-like inter-subunit reorganization of the ribosome during translocation. *Nature* **406**, 318–322 (2000).
3. L. H. Horan, H. F. Noller, Intersubunit movement is required for ribosomal translocation. *Proc. Natl. Acad. Sci. U.S.A.* **104**, 4881–4885 (2007).
4. C. M. T. Spahn *et al.*, Domain movements of elongation factor eEF2 and the eukaryotic 80S ribosome facilitate tRNA translocation. *EMBO J.* **23**, 1008–1019 (2004).
5. A. H. Ratje *et al.*, Head swivel on the ribosome facilitates translocation by means of intra-subunit tRNA hybrid sites. *Nature* **468**, 713–716 (2010).
6. P. V. Cornish, D. N. Ermolenko, H. F. Noller, T. Ha, Spontaneous intersubunit rotation in single ribosomes. *Mol. Cell* **30**, 578–588 (2008).
7. D. N. Ermolenko *et al.*, Observation of intersubunit movement of the ribosome in solution using FRET. *J. Mol. Biol.* **370**, 530–540 (2007).
8. Z. Guo, H. F. Noller, Rotation of the head of the 30S ribosomal subunit during mRNA translocation. *Proc. Natl. Acad. Sci. U.S.A.* **109**, 20391–20394 (2012).
9. D. J. F. Ramrath *et al.*, Visualization of two transfer RNAs trapped in transit during elongation factor G-mediated translocation. *Proc. Natl. Acad. Sci. U.S.A.* **110**, 20964–20969 (2013).
10. J. Zhou, L. Lancaster, J. P. Donohue, H. F. Noller, Crystal structures of EF-G-ribosome complexes trapped in intermediate states of translocation. *Science* **340**, 1236086 (2013).
11. J. Zhou, L. Lancaster, J. P. Donohue, H. F. Noller, How the ribosome hands the A-site tRNA to the P site during EF-G-catalyzed translocation. *Science* **345**, 1188–1191 (2014).
12. N. Inoue-Yokosawa, C. Ishikawa, Y. Kaziro, The role of guanosine triphosphate in translocation reaction catalyzed by elongation factor G. *J. Biol. Chem.* **249**, 4321–4323 (1974).
13. C. E. Cunha *et al.*, Dual use of GTP hydrolysis by elongation factor G on the ribosome. *Translation (Austin)* **1**, e24315 (2013).
14. J. B. Munro, M. R. Wasserman, R. B. Altman, L. Wang, S. C. Blanchard, Correlated conformational events in EF-G and the ribosome regulate translocation. *Nat. Struct. Mol. Biol.* **17**, 1470–1477 (2010).
15. A. Savelsbergh, M. V. Rodnina, W. Wintermeyer, Distinct functions of elongation factor G in ribosome recycling and translocation. *RNA* **15**, 772–780 (2009).
16. M. V. Rodnina, A. Savelsbergh, V. I. Katunin, W. Wintermeyer, Hydrolysis of GTP by elongation factor G drives tRNA movement on the ribosome. *Nature* **385**, 37–41 (1997).
17. J. Chen, A. Petrov, A. Tsai, S. E. O'Leary, J. D. Puglisi, Coordinated conformational and compositional dynamics drive ribosome translocation. *Nat. Struct. Mol. Biol.* **20**, 718–727 (2013).
18. C. Chen *et al.*, Elongation factor G initiates translocation through a power stroke. *Proc. Natl. Acad. Sci. U.S.A.* **113**, 7515–7520 (2016).
19. L. Yao, Y. Li, T.-W. Tsai, S. Xu, Y. Wang, Noninvasive measurement of the mechanical force generated by motor protein EF-G during ribosome translocation. *Angew. Chem. Int. Ed. Engl.* **52**, 14041–14044 (2013).
20. H. Yin, M. Gavriliuc, R. Lin, S. Xu, Y. Wang, Modulation and visualization of EF-G power stroke during ribosomal translocation. *ChemBioChem* **20**, 2927–2935 (2019).
21. V. Petrychenko *et al.*, Structural mechanism of GTPase-powered ribosome-tRNA movement. *Nat. Commun.* **12**, 5933 (2021).
22. R. K. Agrawal, A. B. Heagle, P. Penczek, R. A. Grassucci, J. Frank, EF-G-dependent GTP hydrolysis induces translocation accompanied by large conformational changes in the 70S ribosome. *Nat. Struct. Biol.* **6**, 643–647 (1999).
23. A. Savelsbergh *et al.*, An elongation factor G-induced ribosome rearrangement precedes tRNA-mRNA translocation. *Mol. Cell* **11**, 1517–1523 (2003).
24. F. Peske, A. Savelsbergh, V. I. Katunin, M. V. Rodnina, W. Wintermeyer, Conformational changes of the small ribosomal subunit during elongation factor G-dependent tRNA-mRNA translocation. *J. Mol. Biol.* **343**, 1183–1194 (2004).
25. W. Holtkamp *et al.*, GTP hydrolysis by EF-G synchronizes tRNA movement on small and large ribosomal subunits. *EMBO J.* **33**, 1073–1085 (2014).
26. M. V. Rodnina, F. Peske, B.-Z. Peng, R. Belardinelli, W. Wintermeyer, Converting GTP hydrolysis into motion: Versatile translational elongation factor G. *Biol. Chem.* **401**, 131–142 (2019).
27. A. S. Spirin, The ribosome as a conveying thermal ratchet machine. *J. Biol. Chem.* **284**, 21103–21119 (2009).
28. J. Frank, R. L. Gonzalez Jr., Structure and dynamics of a processive Brownian motor: The translating ribosome. *Annu. Rev. Biochem.* **79**, 381–412 (2010).
29. T. Liu *et al.*, Direct measurement of the mechanical work during translocation by the ribosome. *eLife* **3**, e03406 (2014).
30. E. Salsi, E. Farah, D. N. Ermolenko, EF-G activation by phosphate analogs. *J. Mol. Biol.* **428** (10 Pt B), 2248–2258 (2016).
31. M. R. Wasserman, J. L. Alejo, R. B. Altman, S. C. Blanchard, Multiperspective smFRET reveals rate-determining late intermediates of ribosomal translocation. *Nat. Struct. Mol. Biol.* **23**, 333–341 (2016).
32. C. E. Carbone *et al.*, Time-resolved cryo-EM visualizes ribosomal translocation with EF-G and GTP. *Nat. Commun.* **12**, 7236 (2021).
33. E. J. Rundlet *et al.*, Structural basis of early translocation events on the ribosome. *Nature* **595**, 741–745 (2021).
34. K. Fredrick, H. F. Noller, Catalysis of ribosomal translocation by sparsomycin. *Science* **300**, 1159–1162 (2003).
35. V. I. Katunin, A. Savelsbergh, M. V. Rodnina, W. Wintermeyer, Coupling of GTP hydrolysis by elongation factor G to translocation and factor recycling on the ribosome. *Biochemistry* **41**, 12806–12812 (2002).
36. D. N. Ermolenko, H. F. Noller, mRNA translocation occurs during the second step of ribosomal intersubunit rotation. *Nat. Struct. Mol. Biol.* **18**, 457–462 (2011).
37. R. Belardinelli *et al.*, Choreography of molecular movements during ribosome progression along mRNA. *Nat. Struct. Mol. Biol.* **23**, 342–348 (2016).
38. R. Belardinelli, M. V. Rodnina, Effect of fusidic acid on the kinetics of molecular motions during EF-G-induced translocation on the ribosome. *Sci. Rep.* **7**, 10536 (2017).
39. M. Levi, K. Nguyen, L. Dukaye, P. C. Whitford, Quantifying the relationship between single-molecule probes and subunit rotation in the ribosome. *Biophys. J.* **113**, 2777–2786 (2017).
40. S. M. Studer, J. S. Feinberg, S. Joseph, Rapid kinetic analysis of EF-G-dependent mRNA translocation in the ribosome. *J. Mol. Biol.* **327**, 369–381 (2003).
41. J. A. Dunkle *et al.*, Structures of the bacterial ribosome in classical and hybrid states of tRNA binding. *Science* **332**, 981–984 (2011).
42. R. Belardinelli, H. Sharma, F. Peske, M. V. Rodnina, Perturbation of ribosomal subunit dynamics by inhibitors of tRNA translocation. *RNA* **27**, 981–990 (2021).
43. D. Niblett *et al.*, Mutations in domain IV of elongation factor EF-G confer -1 frameshifting. *RNA* **27**, 40–53 (2021).
44. E. Salsi, E. Farah, J. Dann, D. N. Ermolenko, Following movement of domain IV of elongation factor G during ribosomal translocation. *Proc. Natl. Acad. Sci. U.S.A.* **111**, 15060–15065 (2014).
45. G. Demo *et al.*, Structural basis for +1 ribosomal frameshifting during EF-G-catalyzed translocation. *Nat. Commun.* **12**, 4644 (2021).
46. K. Abel, F. Jurnak, A complex profile of protein elongation: Translating chemical energy into molecular movement. *Structure* **4**, 229–238 (1996).
47. W. Holtkamp, W. Wintermeyer, M. V. Rodnina, Synchronous tRNA movements during translocation on the ribosome are orchestrated by elongation factor G and GTP hydrolysis. *BioEssays* **36**, 908–918 (2014).
48. J. Zhou, L. Lancaster, J. P. Donohue, H. F. Noller, Spontaneous ribosomal translocation of mRNA and tRNAs into a chimeric hybrid state. *Proc. Natl. Acad. Sci. U.S.A.* **116**, 7813–7818 (2019).
49. Y. Kaziro, The role of guanosine 5′-triphosphate in polypeptide chain elongation. *Biochim. Biophys. Acta* **505**, 95–127 (1978).
50. Y.-G. Gao *et al.*, The structure of the ribosome with elongation factor G trapped in the posttranslocational state. *Science* **326**, 694–699 (2009).
51. A. F. Brilot, A. A. Korostelev, D. N. Ermolenko, N. Grigorieff, Structure of the ribosome with elongation factor G trapped in the pretranslocation state. *Proc. Natl. Acad. Sci. U.S.A.* **110**, 20994–20999 (2013).
52. B.-Z. Peng *et al.*, Active role of elongation factor G in maintaining the mRNA reading frame during translation. *Sci. Adv.* **5**, eaax8030 (2019).
53. J. Flis *et al.*, tRNA translocation by the eukaryotic 80S ribosome and the impact of GTP hydrolysis. *Cell Rep.* **25**, 2676–2688.e7 (2018).

54. K. Caban, R. L. Gonzalez Jr., The emerging role of rectified thermal fluctuations in initiator aa-tRNA- and start codon selection during translation initiation. *Biochimie* **114**, 30–38 (2015).
55. D. Hughes, J. F. Atkins, S. Thompson, Mutants of elongation factor Tu promote ribosomal frameshifting and nonsense readthrough. *EMBO J.* **6**, 4235–4239 (1987).
56. E. Vijgenboom, L. Bosch, Translational frameshifts induced by mutant species of the polypeptide chain elongation factor Tu of *Escherichia coli*. *J. Biol. Chem.* **264**, 13012–13017 (1989).
57. S. Tapio, C. G. Kurland, Mutant EF-Tu increases missense error in vitro. *Mol. Gen. Genet.* **205**, 186–188 (1986).
58. R. M. Voorhees, V. Ramakrishnan, Structural basis of the translational elongation cycle. *Annu. Rev. Biochem.* **82**, 203–236 (2013).
59. R. Weiss, J. Gallant, Mechanism of ribosome frameshifting during translation of the genetic code. *Nature* **302**, 389–393 (1983).
60. H. S. Zaher, R. Green, Quality control by the ribosome following peptide bond formation. *Nature* **457**, 161–166 (2009).
61. H. S. Zaher, R. Green, A primary role for release factor 3 in quality control during translation elongation in *Escherichia coli*. *Cell* **147**, 396–408 (2011).